

CHAPTER 1

MELTING A

1.1 Background: melting

11.1 Theories of melting, 3D, 2D, bulk

3D crystals w/ stable surfaces melt from within via Born melting

or yet another strike.

2 Large crystals melt by two-step process via hexatic phase

2D finite crystals melt from perimeter

• if melt from perimenter, dN/dt goes as $N^{1/2}$

1.12 Expectations for 2D finite crystals

1.2 Experiment of Savage et. al

1.2.1 Setup

12.2 Treadle Depletion potential

Results

2. *Intervista* *alla* *prof.* *Anna* *Costa*

$$b. \langle \psi | \hat{O}^2 | \psi \rangle \text{ vs. } \langle \psi | \hat{O} | \psi \rangle^2$$

C. vs. N, by layer

d. No dependence of fast-melting feature on initial cluster size or melting rate

13 Simulations

131 Motivation Motivation

Rule out any hydrodynamic effects causing fast-melting

b. Determine whether range of potential plays role in fast melting

13.2 Justification for using Brownian dynamics

133 GRAMS Simulations

a. *Brownian dynamics* option

b. Equation of motion:

$$\bullet \quad \frac{d^2 r_i}{dt^2} = - \sum_j \frac{\partial U(r_{ij})}{\partial r} - \Gamma \frac{dr_i}{dt} + M_i(t)$$











c. Interparticle depletion potential

opinions that inspire it

$$\bullet \quad U(r) = 4/r(10r - 9)^{1/2} - 400a_0(r - r_0)^2 \text{ for } r \leq r_0$$









d. Temperature

e. Effective well depth: $3.5k_B T$

f. Time step: 2.5×10^{-5} (in GROMACS time units)

g. $N = 100$ particles

h. periodic box of size $L=18.0\sigma$

1. particle area fraction of 24%

13.4 Simulated Depletion Potential

2. A-Model Model

Leinard-Jones repulsion, to avoid dissipation in simulation

c. *Minic* that in *experiment* *minic*

$$d. \quad U(r) = 0 \text{ for } r > r_0$$

$$\text{e. } U(r) = 4/(10r - 9)^{1/2} - 40a_0(r - r_0)^2 \text{ for } r \leq r_0$$









135 Simulated Land-Use Potential

13.6 Results

2. *Intervista* *alla* *signora* *Anna* *Costa*

$$b. \langle \psi | \hat{O}^2 | \psi \rangle \text{ vs. } \langle N | \hat{O}^2 | N \rangle$$

C. vs. N, by layer

1. mean-square fluctuations in bond lengths

e.N vs.t for Leonard-Jones potential

Phase diagram showing lack of first-order potential

137
Discussion Discussion

CHAPTER 2

MELTING B

2.1 Background

2.1 Colloids: macroscopic systems analogous to atomic systems

2. *sinilites*: *sinilitis*

Please provide your position

can investigate atomic behavior via analog

by difference: $1000 - 100 = 900$

novel and phobias

superheated steam boiler

interpretational reading

2.1.2 Experiment by Savage et al: no melting kinetics

a. system: hard spheres with short-range attraction (relative to diameter)

1b. experiment details

c. two-stage melting process

first melts from peritectic reaction critical size

- then breaks up into dense amorphous phase, which is unstable and rapidly evaporates

cross-over circuit at typical magnetic field

experiments: magnetic size 20-30 particles

initialations: magic size 40-50 particles

little dependence on temperature

no dependence on temp in simulation?

1. Several possible explanations are revealed on it:

- 'fast melting' behavior means rate not limited by thermal breaking of bonds

W12)

- density decreases as crystallites shrink: melting kinetics not governed by surface tension

definitely behavior not history dependent

not classical nucleation of liquid within solid below critical crystal size

2.1.3 *Over hypothesis: thermally-activated defects enhance melting rate*

adventitious

experience of discrimination leads to creation of stress

criticism can be released through propagation of cracks

does propagate or not depending on potential

short-range, 'brittle' potential allows to propagate

longer-range, 'ductile' potential

$g_s(\omega)$ is notion of a 'crack' in a liquid droplet sensible?

2.1.4 Evidence for hypothesis

Disciplines are implicated in breakup

• GROMACS BBD simulations, using depletion-like potential (from Part A)

• *exhibit fast-melting (from Part A)*

order parameter decreases sharply (Part A)

average disinflation' reaches $+1$ at the magic size

Disclination and twinning affected by range of potential

Over BID simulations with screened Covid potential

Time range of potential, short- and long-range (amb values?)

• Short-range: x percent fast melting; long-range: y percent fast melting; $x \ll y$

2.1.5 Background Theory

Energy cost for creating a disinflation

Assume flat 2D membrane w/ Young's modulus Y , etc

Retired

Griffith criterion for spontaneous crack propagation

Assume each letter, 1

potential energy of the sheet,

surface irregularities, V

of the world

• Crack is perpendicular to circumferential component $\sigma_{\theta\theta}$ of the disclination induced mechanical stress

• Potential energy of the sheet: $V = -\frac{\pi \ell^2 \sigma \theta^2 (1-v^2)}{4Y} + 2\gamma \ell + V_0$

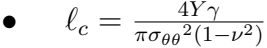
0 is the Bird

● *vis* is the *vis*ing's mod*vis*is

γ is the surface energy per unit length

$\frac{1}{2} \rho v^2$ is the elastic energy in the absence of any cracks, or applied stress

c. Minimize V , get: Minimize



$$\sigma_{\text{tot}} = \frac{4\pi}{\pi \sigma_{\text{tot}}^2 (1 - v^2)}$$

Cracks with length \geq will grow over their energy

Cracks with length > 1 will heal

d. 'Hoopstresses': $\sigma_{\theta\theta}$

• Hopster's catch to open up

• Obtain it from Airy stress function $\chi(r)$ [?] at a distance r from a positive disclination at the center of a two dimensional membrane of radius R

$$\chi(r) = \frac{y_0}{8\pi r^2} \left(\ln \frac{r}{R} - \frac{1}{2} \right)$$

The hoop stress is the circumferential component of the stress tensor σ


• Given by $\sigma_{\theta\theta} = \frac{\partial^2 \chi}{\partial r^2} = \frac{Y}{12} \left(1 + \ln \frac{r}{R} \right)$.

e. When critical crack length is $\tilde{c} =$ a lattice spacing, even a single discli-

nation can rupture crystallite.



Substituting ρ in expression for critical size, we get:



$$e_c = \frac{4Y\gamma_{144}}{\pi(1-v^2)Y^2(1+\ln\frac{r}{R})^2} \approx \frac{576\gamma}{\pi Y}$$

aspiring scientists

So, when $\gamma > \gamma_c$, the probability of the crystal rupturing is greater.

g. Estimation of γ and γ for our system

$$\begin{aligned}
 & \bullet \\
 & \mathbf{V} = -\frac{2}{\sqrt{3}} \mathbf{U}'' \left(\mathbf{x} \right) \Big|_{\mathbf{x} = 0}
 \end{aligned}$$

• where a is equilibrium separation between the particles forming cluster

consider a hexagonal cluster with each side of dimension $1/d$

distance of an interfacial line from the center of mass of the cluster is proportional to the interfacial energy of this line

• Therefore, $\gamma M \frac{\sqrt{3}}{2} a = 6 M U(a)$ becomes $\gamma = \frac{4 \sqrt{3} U(a)}{a}$

So, critical length $\ell_c \approx \frac{-576 \times 6}{\pi a} \frac{V(a)}{V'(a)}$

h. Resulting predictions:

for the depletion potential, $\epsilon = 0.35$

• for screened coulomb, for the potential in Eq.(??), $l_c \approx \frac{1100}{a} \frac{\lambda^2(a-\sigma)}{-a+\sigma+2\lambda}$
 where $a = \lambda + \sigma$

when $\alpha = 1$ and $\lambda = 0.2$, the critical crack length is very large: $l_c \approx 30.6$

• when $\lambda = 0.014$, the critical crack length is a fraction of the lattice spacing, *viz*, $l_c \approx 0.21a$

- Only a single net disclination required to rupture cluster for short-range potential

i. the energy required to introduce a disclination at the center of the

crystallite is $E \approx 0.0014NU_0(\lambda + \sigma)^2/\lambda^2$, for the potential in Eq.??

j. cost of introducing a disinclination is $1/\lambda^2$ for $\sigma \geq \lambda$

kineticist increase rapidly with decreasing potential range

1. suggests the existence of a lower bound on the range of the potential
for thermal activation of disclinations

m. These two competing effects imply that the crossover in the melting rate can arise due to the presence of disclinations only at an optimum range of values for the range of the inter-particle interaction potential

2.2 Methods

22.1 Re-analyze data from GROMACS, Part A

222 New Brownian Dynamics Simulation Code

and Screened Double Potential

$$\bullet \quad U(r) = \frac{U_0(r - \sigma)}{\lambda} e^{-(r - \sigma)/\lambda}$$

b. Equation of motion: $\frac{d^2 r_i}{dt^2} = - \sum_j \frac{\partial U(r_{ij})}{\partial r} - \Gamma \frac{dr_i}{dt} + V_i(t)$











c. Random number generator: Gaussian distr.

1. Cell method for nearest neighbor determination

e. Periodic boundary conditions

2.2.3 Analysis methods

a. Criterion for 'break in slope'

b. Finding the melting temperature

Generating 'equilibrium' initial configurations

1. Determining the dislocation charge

voronoi, Delaunay, code

2.3 Results/Figures

23.1 IN vs t

23.2 Order vs. IN Order

2.3.3 Breakdown by layers

2.3.4 Average disclination charge

2.3.5 Phase diagram for various ranges of potential

2.4 Discussion Discussion

CHAPTER 3

DIAMETER OF RANDOM CLUSTERS

3.1 Introduction

3.1.1 Potts Model [?]

a. Generalization of Ising Model to q spin states

b. Applications

containing Fieldwork

Perpetui Indivisi

not in

What the Bible says

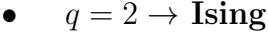
Computer Intelligence



$$\text{c. } H = -K \sum_{\langle i,j \rangle} \delta_{\sigma_i, \sigma_j}$$

d. Rich phase diagram

Maped onto Random Cluster model for $q \geq 0$



f. For $q \leq 4$, the model exhibits a second-order phase transition at the critical point

g. For $q > 4$, the transition is first order[?]

312 Chemical Distance

Until recently, only studied for Potts $q=1$

b. Scaling: $\propto r^{d_{min}}$

c. We extend study to $q=1, 2, 3, 4$ 2D Potentials Model

1. Use S-V algorithm to generate bonds, clusters

End Border Respond to spin color relation via Random Color Model

313 Diameter

a. w , which we define as the longest of all the shortest paths between
sites on a cluster

b. Applications/connections

mainframe

coloration

● *Scandinavia* *vs* *Scandinavian*

c. hypothesis: d_{min} equal to v_{min}

d. Algorithm

• Finding all-pairs shortest paths as $\mathcal{O}(N^2)$

on the subject, more efficient and

e. Mean Field predictions

At or above critical diam, ME should apply

• underlying graph of connected sites that form the critical cluster should be well approximated by a complete graph of n vertices

- complete graph: simple graph in which every pair of vertices is connected by an edge

• Shown by Nachmias [?] that diam of complete graph at criticality scales as $w(n) \propto n^{1/3}$

test We simulate $q=2$, $D=4$ Pots to assess MFT predictions

- Since the mapping of the complete (linear) graph to the Potts random graph in 4D is $L^4 = n$, $w(L) \propto L^{4/3}$; thus, we may expect that w_{min} should equal $4/3$ for $q = 2$ in $4D$.

3.2 Methods

3.2.1 Sverdrup-Vang Algorithm

a. *SV* algorithm [?] used to generate statistics for models, create the

bond-paths studied here

b. Based on work of Fortuin and Kasteleyn[?]

C. Procedure:

• Introduce bonds with probability $p(\sigma_i, \sigma_j) = \delta_{\sigma_i, \sigma_j} (1 - e^{-K})$

Created with Goodnotes

Choose one of q possible spin states and assign to all sites in the

d. Reduces critical slowing relative to algorithms that flip individual

spins [?], e.g. Metropolis algorithm [?]

e. Bonds introduced in SV algorithm correspond to correlations among spins

l. We study paths along bonds in these clusters

3.2.2 Determining the Chen Distance and Diameter

Review of Previous Methods Review

Stanley, Grasseberger[?], Leath, Paul[?], etc.

Mentory considerations, two seeds, etc.

b. Leaf growth [?]

- using a random number generator, one assigns all the bonds associated with the seed site the status “occupied” or “unoccupied” with probability p

- If a bond is assigned ‘occupied’ status, the site to which this bond connects is deemed a ‘growth site’, and is added to cluster.

• All the sites thus added to the cluster in this round form a ‘chemical shell’ of distance r from the seed site.

- This process is then continued for subsequent generations of growth trials, each associated with a larger chemical shell; the growth process stops naturally when one of the growth rounds generates no new growth sites.

- (Note: sites not added to the cluster in a particular round get another chance to be added to the cluster in subsequent rounds; but, once added, are no longer considered as possible growth sites.)

Least growth must appropriate for what we're measuring

Can't use two-seed method; we must find all possible paths

3.2.3 Procedure for $q \geq 1$

a. Generate a new cluster configuration using the Swendsen-Wang algorithm (see above) with periodic boundary conditions. The identification of connected clusters in this steps allows us to determine the largest cluster in the system.

board and on site. This is the best site.

c. Beginning with the seed site s , determine all sites in the largest cluster by “growing” along satisfied cluster bonds (this process does not change the bonds that were determined in step 1).

d. The chemical shell reached in the final step of this growth process, $shell_{final}$, is considered to be the randomly-chosen chemical distance on the largest critical cluster, and is added to our statistics for the chemical distance.

e. All the i sites at the end of this growth process whose nearest neighbors are all occupied are deemed to be perimeter sites, p_i . This set includes all of the external perimeter sites of the cluster.

f. A similar Leath growth process is preformed using each of the perimeter sites as seeds, and $shell_{final_i}$ from each of these growth processes is stored.

g . The diameter for the largest cluster is then $\max\{shel_{j_{max}}, g\}$.

h. This method for finding the diameter is an improvement over the naive N^2 algorithm for solving the all-pairs maximum shortest path problem on the paths formed along cluster bonds. It is expected to scale as $O(pN)$, where p is the number of perimeter sites on the largest critical cluster.

3.2.4 Procedure for $q > 1$

For $q=1$, it is possible to grow a cluster from a seed site.

b. Diameter must have its end points on perpendicular sites

c. Any “pins”, or singly-connected paths on the external perimeter of the cluster, contain sites that can be eliminated as possible diameter endpoints

d. Straightforward to show that the existence of such a “pin” also allows us to eliminate as candidate diameter endpoints that lie within the “body” of the cluster as well

e. 'Proof' / argument for the algorithm:

end: the set of all sites on the pin

- p_{tip} : the site that is the outermost tip of a given pin (i.e., the site with only one nearest neighbor) and p_{attach} the site that attaches this pin to the body of the cluster (i.e., a site with more than 2 nearest neighbors)

- Imagine that we were to include as a candidate site in S some site from P that was not p_{tip} , resulting in a candidate diameter D' ; it would be immediately clear that rejecting this site in favor of p_{tip} would result in a new candidate diameter $D'' > D'$. We can therefore exclude all sites in P that are closer than p_{tip} to S .

- (?) Similar considerations [PROVE THIS?] allow us to additionally exclude from S all sites in N that have a chemical distance from p_{attach} less than or equal to the chemical distance between p_{tip} \mathbf{p}_{attach} (i.e., the length of the pin).

- Initiate, for every site s in S , a “Leath growth” search that examines the chemical distance between s and every other site on the cluster, terminating when all cluster sites have been examined.

D. The maximum chemical distance found across all such searches is then

- We thus need only consider a relatively small proportion [quantify this proportion, on average] of cluster sites as possible diameter endpoints, greatly reducing the number of “Leath scans” required in order to determine the diameter exactly

- Note that this method does not work for periodic boundary conditions,

however; we must therefore grow clusters from a seed site, retaining only those clusters that do not grow to touch the boundaries of the lattice.

if Proceeds Proceeds

Choose a growth site in the center of the lattice

- Perform a Leath growth from this site until the cluster dies, or reaches the boundaries of the maximum lattice size of L_{max} . If any cluster site borders L_{max} , begin again at step 1.

- Identify all the perimeter sites in the cluster by choosing all sites in the final growth step that are perimeter sites (i.e., those that have less than the maximum number of allowed nearest neighbors). In this geometry, all the sites in the final chemical shell will be external perimeter sites.

- Identify all the “pins” among these perimeter sites by performing a
Leath growth from each pin site until one finds a site that is not singly-
connected. All of the sites in the “neck” of the pin are eliminated from
consideration as diameter endpoints.

- Beginning from the point of attachment of the pin to the body of the cluster, continue the Leath scan until one has achieved a chemical shell equal to the distance (along sites) between the point of attachment and the end of the pin. All of sites thus scanned are also eliminated from consideration as diameter endpoints.

- Perform Leath growths from all of the remaining perimeter sites p_i , collecting the maximum chemical shells reached in each instance; the largest of these chemical shells is then the diameter of the cluster.

g. Comparison with 'regular' Least growth method

- We compared this method to the method described for $q > 1$, and

found that the fraction of perimeter sites eliminated as candidates for diameter endpoints was approximately $X\%$ in our runs with $L_{max} = XX$.

h. Label update procedure



325 Simulation Details

2. Overview

• We used the Swendsen-Wang algorithm to simulate Potts Models 2D at criticality for values of L between 8 and L_{max} for our measurements of l , and 4 and L_{max} for our measurements of w . For $q = 2$ in 4D, L ranged between 4 and L_{max3} . All simulations began in a random configuration.

b. values of p_{add} used

• For $q = 1$ in 2D, p_{add} is known exactly (REF). For $q = 2, 3, 4$ in 2D,

$p_{add} = X$ (REF), X (REF), and X (REF), respectively. For $q = 2$ in 4D,

$p_{add} = X$ (REF).

Herminia

- For $q > 1$, the simulations require some time to achieve an equilibrium state, and should therefore be thermalized. Accordingly, each simulation for system size L was run for at least $X_{\tau_{int,m}}$ before measurements were taken, where $\tau_{int,m}$ was the estimated integrated autocorrelation time for the mass of the largest cluster for that value of L .

• A table of integrated autocorrelation times for the largest system sizes measured is provided (Table)

1. *Birds in the*

• In 2D, our simulations were run for a length of $X\tau_{int,m}$; for measurements of v , and for $X\tau_{int,m}$ for measurements of l .

• For our 4D, $q = 2$ measurements, simulations were run for a length of $X_{\tau_{int},m}$ for our measurements of l .

- Some of our simulations consisted of a single, long run; others were the result of combining data from several runs begun from different initial random number generator seeds.

Random Number Generator

- Random numbers for the simulations were generated using the

Mersenne Twister method (REF: Matsumoto + Nishimura 1998), with parameters chosen to provide a period of at least X (determine this)

f. Tests of the algorithm

- As a check on our simulation methods, we also measured the mass of the largest cluster for each lattice size L in order to determine the fractal dimension. The agreement between our values and the latest from the literature was good

g. CPU Time

- The CPU time for simulations measuring the diameter w was approximately $XL^2\mu s$ / iteration; for l it was approximately $XL^2\mu s$ / iteration, when run on the

3.2.6 Data Analysis

a. Blocking Method

• We used the 'blocking' method [?] to extract the proper standard deviation for chemical distance and diameter from measurements.

- This method works by clustering the measurements of the quantity O into blocks of size s ; the average of O is then found for each block independently; the standard deviation in O is then taken to be the standard deviation in these block averages

• $\sigma = \sqrt{\frac{\langle m^2 \rangle - \langle m \rangle^2}{n-1}}$, where n is the number of blocks

b. Fitting Methods

- For $q = 1, 2, 3$, we attempted fits using the Ansätze $y = aL^b$ and $y = aL^b + L/c$, including in the fit data points down to L value of L_{min} , where L_{min} was the smallest value of L that still yielded a reasonable goodness-of-fit value, Q

The fitting form $y = Ax^b$ provided the best fits for all values of q .

• For $q = 4$, we also attempted a fit of the form $y = A + B \log L$; the fit was not as good as the Ansatz $y = aL^b$.

327 Results and Discussion

Comparison, then dist and diameter

b. Comparison of results with those of Deing et.

- Our numerical results appear to match the conjecture of Deng et al. [?] within error for $q = 1$ and $q = 2$; for $q = 3$, we find [wait until results of new blocking analysis are in]. For $q = 4$, we were unable to find a fit of high quality; but our results seem to support Deng et. al's conjecture

c. Discussion of systematic errors

CHAPTER 4

PHASE TRANSITIONS IN COMPUTATIONAL COMPLEXITY

4.1 Background

4.1.1 Constraint Satisfaction Problems (CSP)

a. Examples



Google - Coding in C

Spillies

error-correcting codes

Observation of the hold behavior in CSP

Difficulties in tackling phase behavior of CSP

4.1.2 Proposal: study complexity of percolation model

4.2 Percolation Percol

421 The Model Model Model

4.2.2 Background/applications

43 PRIMA PRIMA

4.3.1 Applications in comp sci

PRIOR CIRCUIT

4.4 Parallel Algorithm for Percolation

4.5 Results

4.5.1 D vs. p for several system sizes L

$$4.5.2 \log(D_2) \text{ vs. } \log(L)$$

43 Distribution of cluster sizes

arithmetic or power law? (power law will often fail)